

Polymer/Additive Compatibility: Study of Primary Antioxidants in PBD

ENIKÖ FÖLDES,¹ JAN LOHMEIJER²

¹ Central Research Institute for Chemistry of the Hungarian Academy of Sciences, H-1525 Budapest, P.O. Box 17, Hungary

² General Electric Plastics bv, 1 Plasticlaan P.O. Box 117, 4600 AC Bergen op Zoom, The Netherlands

Received 21 October 1996; accepted 6 January 1997

ABSTRACT: Stabilization of polymers involves chemical and physical processes, and the effectiveness of antioxidants is strongly influenced by their compatibility with the host system. In the case of rubber-modified high-impact polymer blends, the dispersed elastomer phase is generally the most sensitive to thermooxidative degradation. The compatibility of five hindered phenolic antioxidants with polybutadiene (PBD) was studied as a function of temperature. Relationships were found between the diffusion rate and the specific volume of additive, as well as the total free-volume of the polymer/additive system. The solubility of antioxidants was evaluated on the basis of thermodynamic theories. Deviations from thermodynamic expectations are explained in terms of different physical states and self-association of the substances investigated. © 1997 John Wiley & Sons, Inc. *J Appl Polym Sci* **65**: 761–775, 1997

Key words: polybutadiene (PBD); antioxidant; additive; compatibility; diffusion; transport; solubility

INTRODUCTION

Practically all polymers become into contact with small molecular substances during processing or under service conditions (additives, solvents, gases). The compatibility of an additive with the host polymer is one of the most important parameters determining its effectiveness. Although these materials (processing aids, plasticizers, stabilizers, etc.) belong to the group of small molecules, they are large enough to exhibit physical properties uncharacteristic of common solvents. Earlier studies revealed that most of the antioxidants are polymorphous substances forming different physical structures below their melting point (glassy, different crystal modifications); therefore, their

solubility depends strongly on the thermal history of the polymer/additive system.¹

A wide range of high-performance polymer blends combined of a glassy continuous phase and a dispersed rubber phase has been developed and applied in practice. Polybutadiene (PBD) is one of the elastomers used for toughening. Stabilization of these systems requires special attention to the sensitivity of the double bonds of the rubber phase to thermal and thermooxidative degradation. The thermal degradation of acrylonitrile–butadiene–styrene resin (ABS) begins in the same temperature range as that of PBD.² Relationships were found between the thermooxidative stability of ABS and the degree of PBD grafting, the antioxidant type,³ the PBD content,⁴ as well as the partitioning behavior of additives.^{5,6} Kulich and Wolkowicz⁵ showed that the partitioning is directly correlated with solubility and depends on the composition of the additive and the polymer blend.

In the present work, the diffusion rate and solu-

Correspondence to: E. Földes.

Contract grant sponsor: General Electric Plastics.

Contract grant sponsor: National Scientific Research Foundation of Hungary; contract grant number: OTKA T-019425.

© 1997 John Wiley & Sons, Inc. CCC 0021-8995/97/040761-15

bility of primary antioxidants were studied in PBD. The effects of different parameters (temperature, structure and size of antioxidant, free volume and interaction of the components) on compatibility were investigated.

EXPERIMENTAL

Materials

The experiments were carried out with additive-free polybutadiene (PBD) prepared by emulsion polymerization by General Electric Plastics. After removing all the additives and evaporating water, 200–400 μm -thick films were compression-molded. For the diffusion experiments, disks of 1.8 cm diameter were cut. The polymer is cross-linked and insoluble in any solvent.

Five commercially available primary antioxidants (AO) (Ciba-Geigy products) were studied. The chemical structure and molecular mass (MW) of the materials are given in Table I. Except for AO5, the additives have the same type of hindered phenolic groups. The differences among AO1, AO2, and AO3 are the number of phenolic groups, the length of the coupling ester groups, and the shape of the molecules. The chemical structure of AO4 is similar to that of AO2, except two oxygen atoms of the latter are substituted by NH groups. The structure of AO5 can be compared also to AO2, but on the phenolic groups one of the tertiary butyls is substituted by a methyl, and there are two additional etheric oxygens in the linear chain.

For the diffusion experiments conducted below the melting point of the AO, additive sources were prepared by two methods (PBD-based additive sources):

- The AO was dissolved in a small amount of acetone and mixed with additive-free PBD latex; then, water was evaporated in vacuum at ambient temperature.
- The AO was brought into additive-free PBD film by diffusion process above the melting point of the additive.

Methods

Fourier transform infrared (FTIR) spectroscopy (Galaxy 3020 FTIR spectrophotometer with FIRST Enhanced V1.52 software, *Mattson-unicam*) was used to control the purity of PBD and for characterization of the additives. The glass

transition of the polymer and the physical structure of the additives were studied by differential scanning calorimetry (DSC; Thermal Analysis System TA4000, DSC 30 Measuring Cell, Graph Ware TA72.2/.5 software, *Mettler*) in nitrogen atmosphere as a function of temperature using 10°C/min heating and cooling rate.

The thermal and thermooxidative stabilities of additives were studied by thermogravimetric analysis (TGA; TG 50 unit of the Mettler TA4000 System) under nitrogen and oxygen at a heating rate of 20°C/min, as well as by DSC under oxygen at a rate of 10°C/min. The specific volume of polymer and additives was measured as a function of temperature in liquids by a special dilatometer. Distilled water was used for PBD, and different solvents for the additives (Table IV). The linear thermal expansion of PBD was studied by thermomechanical analysis (TMA; TMA 40 Measuring Cell of the Mettler TA4000 System) in nitrogen atmosphere between ambient temperature and 200°C at a rate of 5°C/min.

The diffusion and solubility of additives in PBD were studied between 15 and 170°C by a sorption technique. Different methods were used below and above the melting point (T_m) of the antioxidants:

- At $T < T_m$, an additive-free PBD film was placed between two "PBD-based additive sources" and AO uptake of the same film was measured as a function of time.
- At $T > T_m$, the PBD film was immersed into melted AO for different times. After the experiment, the film surface was removed by acetone and the AO concentration was determined. A new piece of film was used for each dataset.

The additive content of the samples was measured gravimetrically and controlled by FTIR spectroscopy.

A special process was used to determine the solubility of AO1 at 50°C. An additive-free PBD film was placed between two plates of pure additive prepared by melting and casting onto a glass plate. The system was wrapped in aluminum (Al) foil and stored at 50°C for 1000 h. After the treatment, the excess amount of AO was removed from the surface by acetone.

Note: Although PBD is very sensitive to heat and oxygen, the additive uptake experiments could be carried out in most cases without essential degradation of the polymer (checked by FTIR)

Table I Chemical Composition of AO Investigated

Code	Chemical Structure	MW
A01		531
A02		639
A03		1178
A04		637
A05		587

because of the large excess of primary AO present. Exceptions are discussed in the presentation of the results.

The diffusion coefficient (D) was calculated by the equation given for vapor and liquid uptake by a plane sheet⁷:

$$\frac{M_t}{M_\infty} = 1 - \frac{8}{\pi^2} \sum_{m=0}^{\infty} \frac{1}{(2m+1)^2} \times \exp[-D(2m+1)^2\pi^2 t/l^2] \quad (1)$$

where M_t is the total amount of diffusant absorbed by the sheet at time t ; M_∞ , the equilibrium sorp-

tion amount attained theoretically after infinite time; and l , the thickness of the sheet.

The basic assumptions for the solution of the Fickian diffusion equation by eq. (1) are⁷

- the sheet is free of the diffusant initially;
- the diffusion coefficient is constant;
- the sheet placed into the diffusant immediately attains an equilibrium concentration at each surface which remains constant afterward; and
- the sheet does not swell.

Although the last condition is not fulfilled, as the AO swell PBD, eq. (1) can be used by calculating for a mass-fixed section of the polymer.⁷ For the evaluation of the results, the following transformations were applied in eq. (1):

1. M_t and M_∞ terms were substituted by concentrations, c_t and c_∞ , respectively.
2. The actual sample thickness (l_t) was calculated by eq. (2) and substituted for l :

$$l_t = l_R[1 + (\alpha_0 + \beta c)(T - T_R)] \quad (2)$$

where l_R is the sample thickness measured at room temperature, T_R , before the experiment; α_0 , the linear thermal expansion coefficient of the polymer in absence of the diffusant; c , the concentration of the diffusant in the polymer at temperature T and time t ; and β , the coefficient describing the swelling effect of the diffusant. For determining l_t , the linear thermal expansion coefficient of PBD was measured as a function of AO concentration.

Below the melting point of the additives, two-stage processes were observed. The sorption started with Fickian diffusion followed by a slower first-order kinetics. In the additive source, the diffusant exists partly in dissolved and partly in dispersed solid states. The slower first-order process—following the Fickian diffusion—can be explained by slow dissolution of the dispersed additive. The additive concentration does not remain constant on the surface of the sheet, as the dissolution becomes the rate-determining process in the second stage. For the description of this combined kinetics, a single mathematical model introduced by Berens and Hopfenberg⁸ was used. It is a linear superposition of a phenomenologically independent first-order term upon the ideal Fickian diffusion equation:

$$c_t = c_{t,d} + c_{t,s} \quad (3)$$

where $c_{t,d}$ is the concentration of diffusant absorbed as a result of Fickian diffusion described by eq. (1), while $c_{t,s}$ is that of the diffusant absorbed as a result of a first-order process:

$$c_{t,s} = c_{\infty,s}[1 - \exp(-kt)] \quad (4)$$

where $c_{\infty,s}$ is the equilibrium concentration, and k , the rate constant of first-order kinetics. The equilibrium solubilities and the diffusion rate

were computed by a least-square curve-fitting method.

RESULTS

Characterization of the Polymer

The PBD investigated is an amorphous polymer with a glass transition at -76.8°C . The one-dimensional thermal expansion of the additive-free polymer measured by TMA in nitrogen atmosphere changes linearly between ambient temperature and 150°C . At higher temperatures, thermal degradation starts and is accompanied by crosslinking, resulting in a decrease of the thermal expansion ratio. In the presence of primary AO, the degradation is inhibited and the expansion of the polymer changes linearly in the experimental temperature range.

From the results of the linear thermal expansion coefficient measurements, it was concluded that the volume of the polymer must also change linearly with temperature. The specific volume was measured between 25 and 65°C . The thermal volume expansion coefficient (α_T) and the specific volume extrapolated to absolute zero (v_0) were determined by eq. (5):

$$v_T = v_0(1 + \alpha_T T) \quad (5)$$

where v_T is the specific volume at temperature T . Values of $v_0 = 0.925 \text{ cm}^3/\text{g}$ and $\alpha_T = 6.02 \times 10^{-4} \text{ 1/K}$ were obtained. The extrapolated 0 K specific volume, v_0 , is lower than that predicted by Doolittle⁹ for *n*-paraffin hydrocarbons of infinite molecular weight ($1.0 \text{ cm}^3/\text{g}$) and is close to that of linear polyethylene ($0.912 \text{ cm}^3/\text{g}$) determined by Chiang and Flory.¹⁰ The smaller value of the thermal volume expansion coefficient compared to those measured by Paul and DiBenedetto,¹¹ and calculated by Gee and Boyd¹² for *cis*-PBD, can be attributed to the crosslinking of the PBD investigated.

Characterization of the Additives

The additives investigated can be classified according to the behavior of their OH (and NH) groups: non-hydrogen-bonding and hydrogen-bonding molecules. FTIR studies revealed that AO1–AO3 belong to the first group, while AO4 and AO5, to the second one. Figure 1 shows the FTIR spectra of the solid additives (in KBr) in the O—H and N—H stretching vibration region.

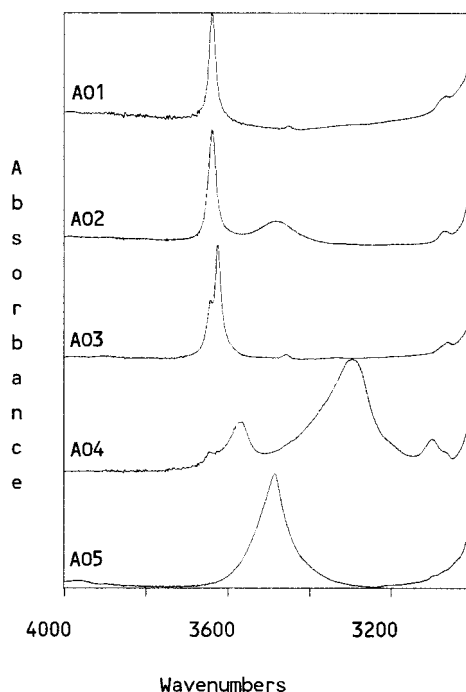


Figure 1 FTIR spectra of crystalline additives ground with KBr.

The unassociated (free) hydroxyl groups absorb in the region $3670\text{--}3580\text{ cm}^{-1}$, giving a sharp band.¹³ As an effect of association, additional broader bands appear at lower frequencies ($3580\text{--}3200\text{ cm}^{-1}$). The free N—H group of secondary amides has a sharp strong band at 3460--

3300 cm^{-1} , which shifts to $3270\text{--}3070\text{ cm}^{-1}$ as a result of interaction. The position of the O—H and N—H bands depends on the strength of hydrogen bonds.¹³

AO1–AO3 give sharp absorption peaks of free OH above 3600 cm^{-1} . AO2 has also a smaller broad band at 3480 cm^{-1} , hinting at the presence of some hydrogen-bonded OH groups, as well. In chloroform or in PBD, the associated OH group absorption of AO2 disappears. FTIR study of AO4 indicates that the OH groups are partly free, partly hydrogen-bonded, while the main part of NH group is hydrogen-bonded. The FTIR characteristics of AO1–AO4 dissolved in PBD are similar to those in the solid state with some frequency shifts, which are higher in the case of associated bands than of free absorptions. The stretching vibration of AO5 is characteristic of hydrogen-bonded OH groups in crystalline and amorphous states, as well as in PBD. In chloroform, AO5 absorbs at 3610 cm^{-1} .

The thermal properties of AO were studied by DSC in nitrogen atmosphere between -50 and 200°C at a rate of $10^\circ\text{C}/\text{min}$ in two heating and cooling runs. The results are summarized in Table II. The additives can also be arranged in two groups according to their thermal behavior measured following melting and cooling.

AO1 crystallizes from the melt during cooling at a rate of $10^\circ\text{C}/\text{min}$. Although the crystallization is not complete, and the melting point (T_m) of

Table II Thermal Properties of AO Measured by DSC in Nitrogen Atmosphere

Additive	Run	Heating			Cooling		
		T_m ($^\circ\text{C}$)	T_g ($^\circ\text{C}$)	ΔH_f (J/g)	T_c ($^\circ\text{C}$)	T_g ($^\circ\text{C}$)	ΔH_c (J/g)
AO1	1	52		133	4		-74
	2	6		75			
		16		-90 ^a			
		51		124			
AO2	1	101		79		0	
	2		0			1	
AO3	1	118		64		44	
	2		50			44	
AO4	1	160		98		54	
	2		55				
AO5	1	80		116		2	
	2		1				

Heating and cooling rate: $10^\circ\text{C}/\text{min}$.

^a Recrystallization.

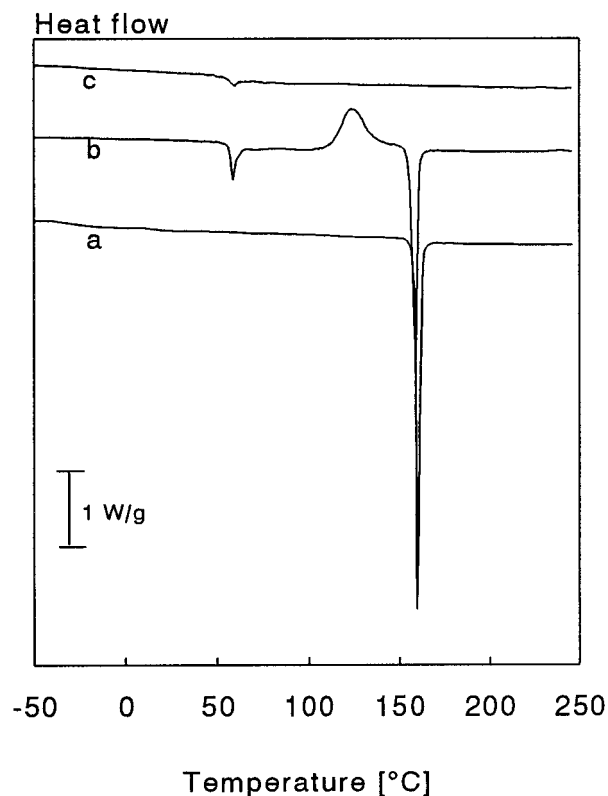


Figure 2 Effect of thermal history on the properties of AO4 studied by DSC at a heating rate of 10°C/min: (a) crystalline material as received; (b) cooled from melt at ambient temperature; (c) cooled from melt to -50°C at a rate of 10°C/min.

the crystals are lower than those of the original substance, the additive recrystallizes either during a second heating run or annealing at ambient temperature.

The four other AO crystallize neither in the course of cooling nor during a second heating run. The supercooled AO2 and AO5 have low glass transition temperatures (T_g) and crystallize at ambient temperature after some annealing time. The process is slower than in the case of AO1 (it takes some weeks). AO3 and AO4 form relatively stable glasses after cooling from the melt with glass transitions around 50°C. Several months are needed for crystallization at ambient temperature. Both substances form several crystal modifications depending on the crystallization conditions. A study on the crystallization characteristics of AO3 was published in ref. 14. The effect of cooling conditions on the fusion characteristics of AO4 is shown in Figure 2 for illustration.

The additives investigated have low volatility and high thermal and thermooxidative self-stabilities. The results of the TGA and DSC studies

(Table III) indicate that all the AO are thermally stable in the temperature range of the experiments.

The specific volumes of additives were measured between 25 and 150°C. The thermal volume expansion coefficients (α_T) calculated and the specific volumes extrapolated to 0 K ($v_{AO,0}$) are given in Table IV. The thermal expansion coefficients of additives are larger and the 0 K specific volumes are smaller than the corresponding values of the polymer.

Diffusion Rate and Solubility

The additive uptake of PBD was measured as a function of time at different temperatures, and the concentrations were plotted as a function of t/l_i^2 . Figure 3 illustrates some results obtained at 140°C (above the melting points of additives) showing the experimental points and the fitted curves. The two-stage diffusion processes experienced under the additive melting point are exemplified in Figure 4 for AO1 and in Figure 5 for AO3. The diffusion rates measured at different temperatures are summarized in Table V, and the solubilities, in Table VI.

The diffusion coefficient of additives obeys the Arrhenius law, as PBD has no phase transition in the temperature range of the experiments:

$$D = D_0 \exp(-E_D/RT) \quad (6)$$

where D_0 is the preexponential factor, E_D , the activation energy of diffusion; R , the universal gas constant; and T , the temperature.

The results of AO4 and AO5 are shown in an Arrhenius plot in Figure 6 for illustration. The calculated D_0 and E_D values of additives studied are summarized in Table VII.

Table III Thermal and Thermooxidative Stability of Additives

Additive	Starting Temperature of Decomposition (°C)		
	TGA in N ₂	TGA in O ₂	DSC in O ₂
AO1	220	208	224
AO2	211	204	208
AO3	286	216	216
AO4	280	235	257
AO5	221	219	250

Rate of heating: TGA, 20°C/min; DSC, 10°C/min.

Table IV Temperature Dependence of Specific Volume of Additives

Additive	Measuring Liquid	$v_{AO,0}$ (cm ³ /g)	$\alpha_T \times 10^4$ (1/K)
AO1	Sunflower oil	0.807	11.4
AO2	Sunflower oil	0.742	10.2
AO3	Sunflower oil, paraffin oil	0.671	13.0
AO4	<i>N</i> -Ethylformamide	0.803	6.7
AO5	Sunflower oil	0.708	9.3

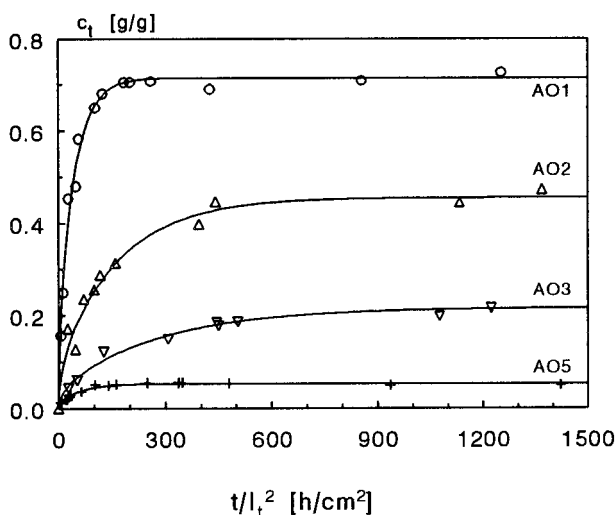
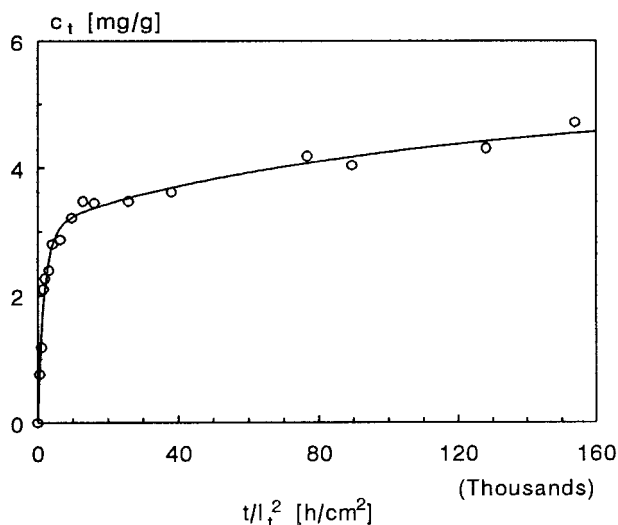
Except for AO4, the solubilities of the additives change also in an Arrhenius mode (Fig. 7), yielding S_0 preexponential factor and E_S activation energy values given in Table VII (in the case of AO1, S_0 and E_S were determined from the solubilities measured between 15 and 50°C). Plotting the activation energies of diffusion and solubility as a function of the preexponential factor, linear relationships are obtained. This phenomenon is quite general in the field of chemical kinetics and is called the "compensation effect."

AO1 has the highest activation energies of diffusion and solubility among the investigated materials. The solubility is extremely high and does not change essentially above the melting point of the additive. This indicates that crosslinks of the polymer prevent complete dissolution in melted AO1.

Comparing the results of AO1, AO2, and AO3 (containing the same chemical groups), an increase of D_0 and E_D with the length of the additive can be observed, but this relationship does not hold for all five substances. The activation energy of AO2 is lower than that of AO1 and higher than

for AO3, although the molecular masses change in reversed order. The smallest activation energies were obtained for AO5 (Fig. 6), the molecular mass of which is between those of AO1 and AO2. These results do not confirm the expectations—based on studies of homologous series—that E_D should increase with the molecular mass of the diffusant (e.g., refs. 15–18). Dudler and Muiños¹⁹ also proved the importance of the shape of the diffusing additives. AO4 has similar diffusion characteristics as those of AO2, but its solubility is extremely small even at high temperatures and $\ln S$ does not change linearly with $1/T$ (Fig. 8).

During the study of AO4 diffusion in PBD, the polymer degraded, as indicated by strong discoloration. The degree of degradation depended on the type of additive source used for the experiments. With discs cast from pure melted additive, the degradation was less pronounced than in the case of the PBD-based additive source. In measuring the additive uptake gravimetrically, a considerable mass increase was observed following a Fickian diffusion step. Beside discoloration, the polymer became brittle. FTIR, DSC, and TMA studies

**Figure 3** Additive uptake of PBD at 140°C.**Figure 4** AO1 uptake of PBD at 15°C.

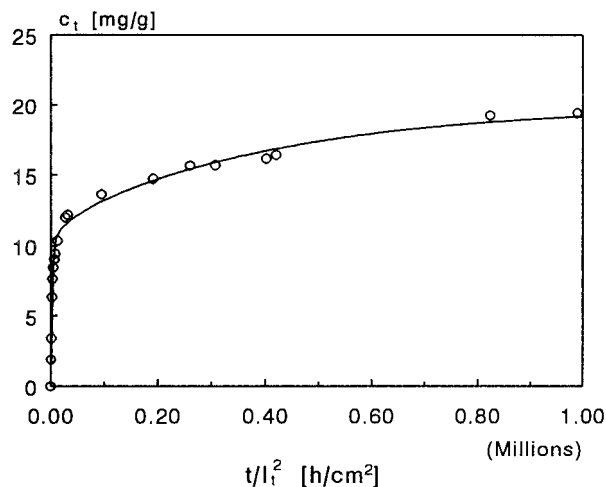


Figure 5 AO3 uptake of PBD at 50°C.

revealed oxidation and crosslinking of the polymer. The rate of early-stage diffusion given in Table V is independent of the additive source type.

Characterization of the Polymer/Additive System

The swelling effect of AO was studied by determining the dimensions of PBD samples at ambient temperature before and after the diffusion experiments. The results showed that the volume of the system changes linearly with additive content.

When the additive concentration is determined in a mass ratio, m_{AO} , the volume ratios can be expressed by

$$\frac{V - V_p}{V_p} = \frac{v_{AO}}{v_p} \frac{m_{AO}}{1 - m_{AO}} \quad (7)$$

where V_p and V are the volumes of the polymer and the polymer/AO system, respectively, and v_p and v_{AO} are the specific volumes of the polymer and additive, respectively.

For illustration, the relative volume changes of the polymer $[\Delta V/V_0]$ is plotted as a function of AO1 ratio $[m_{AO}/(1 - m_{AO})]$ in Figure 9. The slope of the line equals the ratio of specific volumes of AO1 and PBD at room temperature.

Following the high-temperature diffusion experiments, the PBD + AO films lost their transparency at ambient temperature in a more or less long period of time depending on the type of additive. The effect was caused by precipitation of the insoluble part of the additive in the polymer. Separation and crystallization of AO1 in PBD was observed immediately after cooling from high temperature. Figure 10 shows the specific heat of systems containing 8 and 37% w/w AO1, respectively. The first change of specific heat (step on the curve) corresponds to the glass transition of PBD; the fusion peaks at around 50°C originate from the melting of AO1 crystals. The thermal characteristics determined are summarized in Table VIII. The heat of fusion related to the AO1 content of the system is slightly lower than that of the original commercial material (see Table II). The difference is attributed partly to the dissolved fraction and partly to the difference in the surrounding medium during crystallization.

The crystallization of the part causing supersaturation was a much slower process in the other cases. The PBD/AO systems retained their transparency for some time and became gradually hazy during storage at ambient temperature for several months. The specific heat of the compounds containing 3 and 25% w/w AO3 measured 8

Table V Diffusion Rate of Additives in PBD

Temperature (°C)	D (cm ² /s)				
	AO1	AO2	AO3	AO4	AO5
15	$1.57 \cdot 10^{-10}$				
23	$1.00 \cdot 10^{-10}$	$6.86 \cdot 10^{-10}$	$7.42 \cdot 10^{-10}$		
25				$4.41 \cdot 10^{-10}$	$1.76 \cdot 10^{-8}$
35	$2.57 \cdot 10^{-9}$				
50	$1.38 \cdot 10^{-9}$	$2.17 \cdot 10^{-9}$	$7.05 \cdot 10^{-9}$	$5.59 \cdot 10^{-9}$	$5.51 \cdot 10^{-8}$
90				$2.66 \cdot 10^{-8}$	
120				$6.89 \cdot 10^{-8}$	
140	$6.08 \cdot 10^{-7}$	$1.58 \cdot 10^{-7}$	$9.37 \cdot 10^{-8}$		$4.11 \cdot 10^{-7}$
170	$2.08 \cdot 10^{-6}$	$4.82 \cdot 10^{-7}$	$2.23 \cdot 10^{-7}$		$9.90 \cdot 10^{-7}$
180				$4.38 \cdot 10^{-7}$	

Table VI Solubility of Additives in PBD

Temperature (°C)	S (% w/w)				
	AO1	AO2	AO3	AO4	AO5
15	0.6				
23	3.0	0.8	0.4		
25				0.4	0.9
35	7.6				
50	71.5	2.9	1.7	0.4	1.3
90				0.7	
120				0.9	
140	72.0	45.4	21.9		5.5
147	80.0	67.0	26.6		
170	74.7	63.5	27.1		8.0
180				3.4	

months after the high-temperature diffusion experiments are shown in Figure 11. The characteristics of the curves are given in Table VIII. In the presence of PBD, the additive melting point shifts to lower temperature related to the known crystal modifications of AO3.¹⁴

The primary AO investigated separated in the polymer bulk, resulting in hazing, but no special

exudation was observed. Nah and Thomas²⁰ experienced blooming of pure waxes in natural rubber vulcanizates. The rate of blooming was found to be dependent on the modulus of rubber and was attributed to elastic stresses. Our studies on secondary AO revealed—in accordance with Loadman²¹—that the mode of additive precipitation (blooming or crystallization in the polymer bulk) is determined not only by the polymer but also by the additive type.

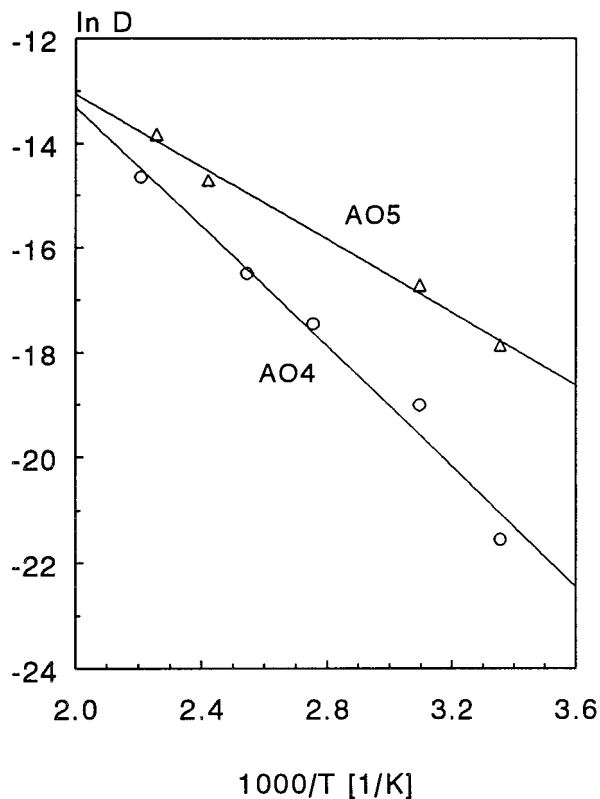


Figure 6 Temperature dependence of additive diffusion in PBD.

DISCUSSION

Parameters Influencing the Rate of AO Diffusion

The results of the diffusion experiments revealed no direct relationship between the activation energy of diffusion and the molecular mass of additive. In an earlier work, the diffusion of additives in ethylene polymers was studied²² and the results were evaluated on the basis of the free-volume theory originally developed by Cohen and Turnbull.²³ According to the theory, the diffusion rate of a small molecule can be described by an exponential function of the fractional free volume (f) of the polymer:

$$D = D_0 \exp(-B_d/f) \quad (8)$$

where B_d is related to the minimum hole size required for the displacement of the diffusant.

It is noted that D_0 and B_d are related to different physical characteristics (size and shape of the diffusant, minimum hole size) in the literature.^{23,24} In all our experiments, these two param-

Table VII Temperature Dependence of Diffusion Rate and Solubility of Additives in PBD

Additive	D_0 (cm^2/s)	E_D (kJ/mol)	S_0 (w/w)	E_S (kJ/mol)
AO1	$1.32 \cdot 10^2$	65	$7.67 \cdot 10^{15}$ ^a	100 ^a
AO2	$3.01 \cdot 10^{-1}$	50	$9.45 \cdot 10^3$	34
AO3	$1.12 \cdot 10^{-2}$	40	$2.82 \cdot 10^3$	33
AO4	$2.38 \cdot 10^{-1}$	49	—	—
AO5	$2.95 \cdot 10^{-3}$	29	$7.63 \cdot 10^0$	17

^a Calculated from the solubilities measured between 15 and 50°C.

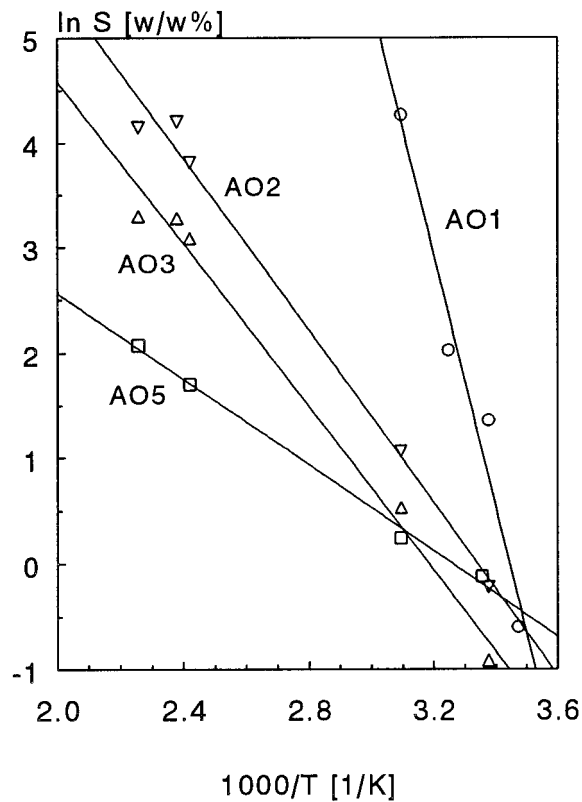
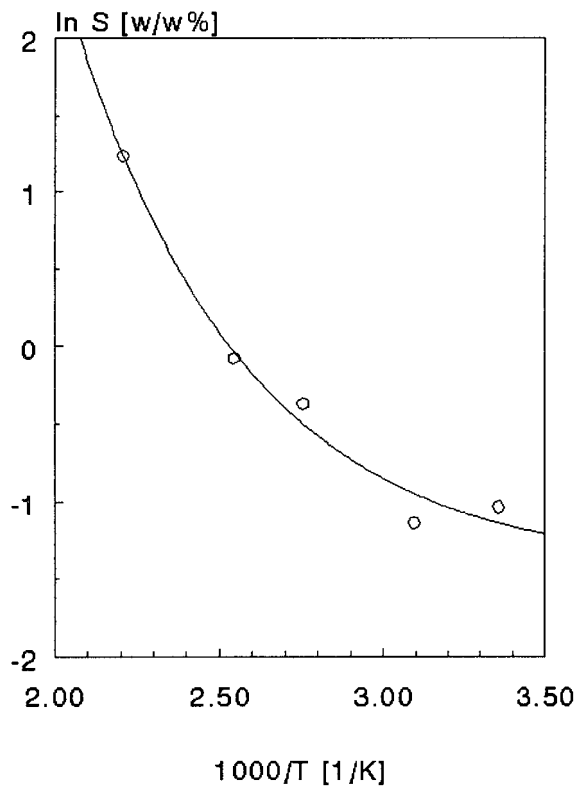
eters are in a linear relationship, indicating that they characterize the same physical phenomenon.

In the case of ethylene polymers, a linear relationship was obtained between the fractional free volume of the noncrystalline phase and the logarithm of the diffusion coefficient.²² Studying the effect of the diffusant structure, good correlation was obtained between the specific volume of the additive and the activation energy of diffusion.

As PBD is an amorphous polymer with low T_g , the free-volume changes linearly with temperature in the range studied. To investigate the effect

of the diffusant structure, the activation energies (E_D) were plotted in Figure 12 as a function of the additive specific volumes (v_{AO}) corresponding to 25°C (calculated from the measured data given in Table IV). E_D increases with v_{AO} , which seems to confirm the general validity of our finding that the specific volume of the penetrant is one of the parameters determining the mobility of additives in polymers.

For further examination, it was considered that the free volume of the polymer increases continuously with that of the penetrating additive. The specific free volumes (v_f) at different tempera-

**Figure 7** Temperature dependence of additive solubility in PBD.**Figure 8** Temperature dependence of AO4 solubility in PBD.

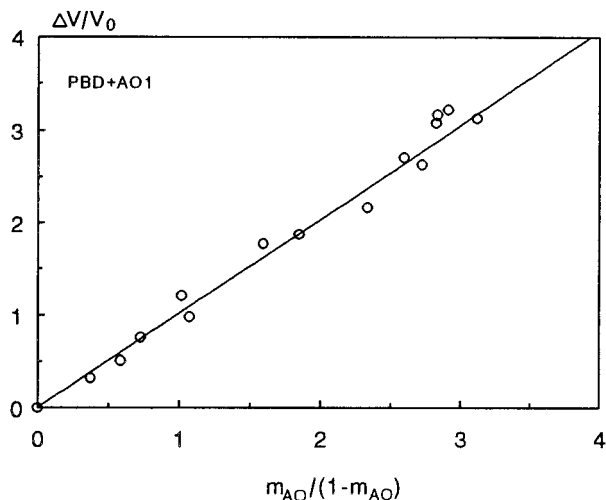


Figure 9 Volume expansion of PBD as a function of additive mass fraction (m_{AO}) at ambient temperature.

tures were calculated from the specific volumes measured (v_T) and the 0 K extrapolated values (v_0) by

$$v_f = v_T - v_0 \quad (9)$$

The overall specific free volume of the polymer/additive system (Σv_f) at a given temperature can be described by the volume fractions (φ_p and φ_{AO}) and the specific free volumes ($v_{f,p}$ and $v_{f,AO}$) of the components:

$$\Sigma v_f = \varphi_p v_{f,p} + \varphi_{AO} v_{f,AO} \quad (10)$$

where indexes p and AO refer to the polymer and AO , respectively.

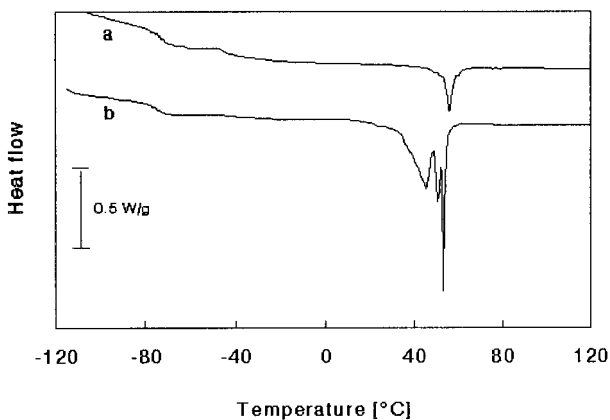


Figure 10 Thermal properties of PBD + AO1 systems measured by DSC at a rate of 10°C/min: (a) 8% w/w AO1; (b) 37% w/w AO1.

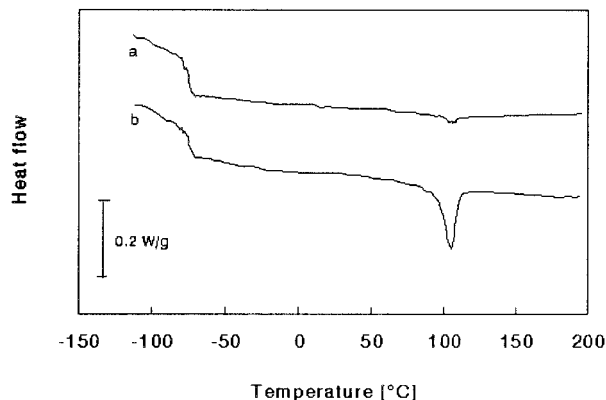


Figure 11 Thermal properties of PBD + AO3 systems measured by DSC at a rate of 10°C/min 8 months after high-temperature diffusion experiment: (a) 3% w/w AO3; (b) 27% w/w AO3.

As the diffusion coefficient calculated by eqs. (1) and (3) corresponds to the moderate and longer times of the process,⁷ the volume fractions of the components at different temperatures were calculated from the total additive uptake values and the specific volumes.

The fractional free volume in eq. (8) was replaced by the overall specific free volume, B by the product of the specific volume of the penetrant at the given temperature (v_{AO}) and a term (A) assumed to be characteristic for the polymer:

$$D = D_{0,p} \exp\left(-\frac{Av_{AO}}{\Sigma v_f}\right) \quad (11)$$

In Figure 13, the logarithm of the diffusion rates are plotted as a function of $v_{AO}/\Sigma v_f$. All the measured data of the different AO scatter around the same line, proving that the specific volume of the penetrant and the overall free volume of the

Table VIII Thermal Properties of PBD + AO Compounds

Additive	c_{AO} (% w/w)	$T_{g,PBD}$ (°C)	$T_{m,AO}$ (°C)	ΔH_{AO}^a (J/g)
AO1	7.9	-72	56	122
AO1	36.9	-76	45	110
			51	
			54	
AO3	3.3	-76	105	63
AO3	25.1	-75	105	46

^a Calculated for the additive content.

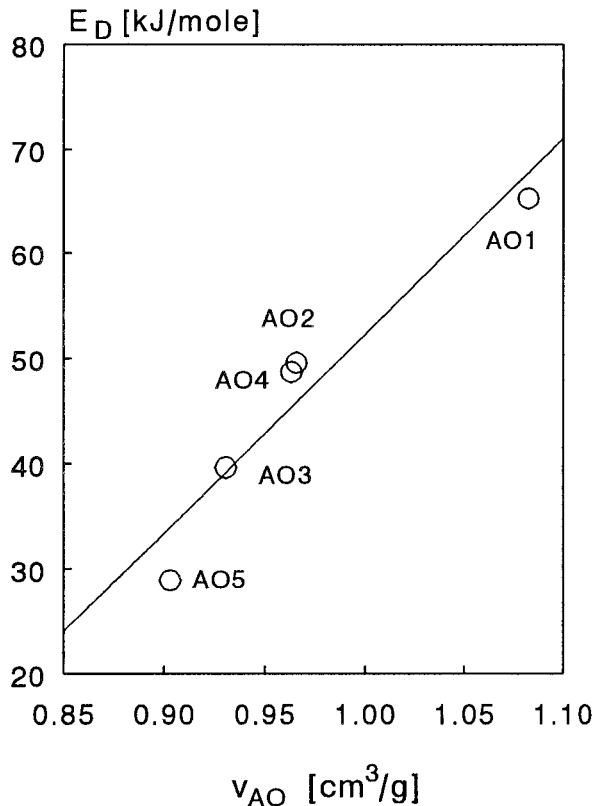


Figure 12 Relationship between the activation energy of diffusion and the specific volume of additives (measured at 25°C) in PBD.

system are two of the controlling parameters in the diffusion of additives above the glass transition of polymers. The third factor is the flexibility of the polymer chains. Equation (11) yields $D_{0,p} = 1.94 \times 10^{-2} \text{ cm}^2/\text{s}$ and $A = 2.83$, values which are considered to be specific for the PBD investigated.

Parameters Influencing AO Solubility

For evaluating the measured solubility values on the basis of the extended thermodynamic theory of the solution of solids,^{1,17,25} the volume fraction of the dissolved additive (φ_{AO}) can be expressed as a function of the heat of fusion of additive and the Flory–Huggins interaction parameter (χ):

$$-\ln \varphi_{AO} = \frac{\Delta H_f}{R} \left(\frac{1}{T} - \frac{1}{T_m} \right) + \varphi_p + \chi \varphi_p^2 \quad (12)$$

where R is the gas constant; ΔH_f , the heat of fusion; T_m , the melting temperature of the additive; and φ_p , the volume fraction of the polymer. Equation (12) is based on the assumption that

the molar volume of the polymer is considerably larger than that of the additive.

The Flory–Huggins interaction parameter can be calculated from the molar volume of the additive (V_{AO}) and the solubility parameters (δ) of the components:

$$\chi = \left(\frac{V_{AO}}{RT} \right) (\delta_p - \delta_{AO})^2 \quad (13)$$

For the calculations, the molar attraction constants given by Hoy²⁶ and the molar volumes determined experimentally were used assuming that χ is concentration- and temperature-independent.

In Figure 14, $-\ln \varphi_{AO}$ is plotted as a function of the right side of eq. (12) for AO1, AO2, and AO3—denoting the first term by H . (Above the melting point of the additive, H is considered zero.) The solubility of AO1 corresponds to the thermodynamically expected values at each temperature under and above T_m . The solubilities of AO2 and AO3 change according to the theoretical

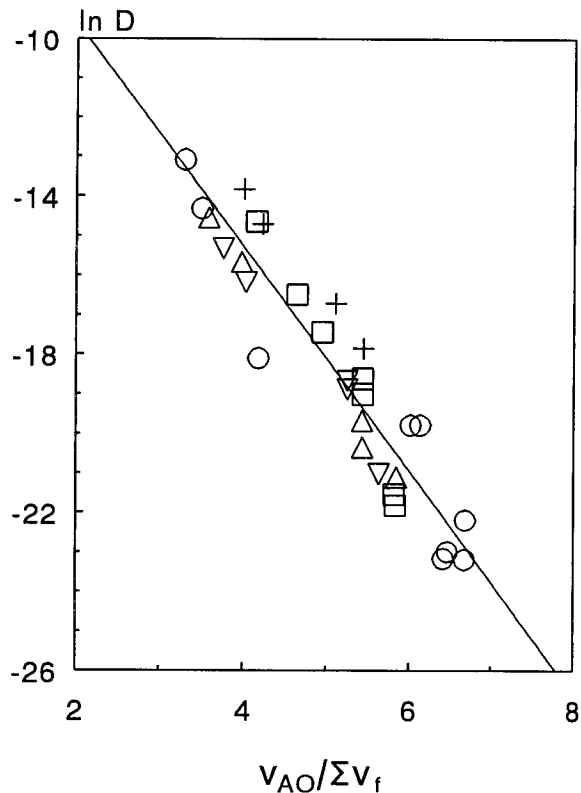


Figure 13 Diffusion rate of additives as a function of specific volume of diffusant related to the free volume of polymer/additive system: (○) AO1; (△) AO2; (▽) AO3; (□) AO4; (+) AO5.

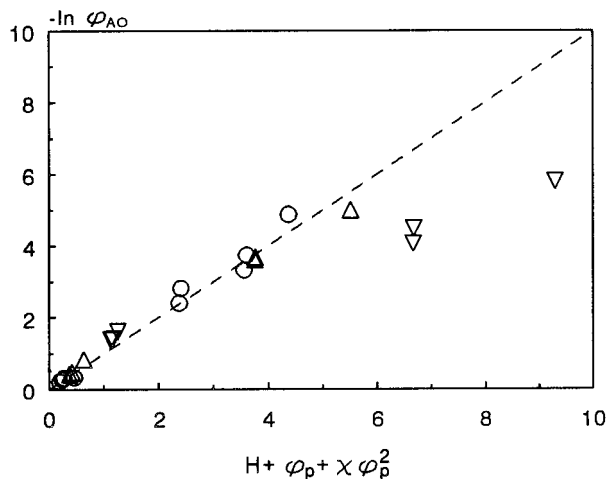


Figure 14 Thermodynamic evaluation of additive solubility in PBD: (○) AO1; (△) AO2; (▽) AO3.

line at $T > T_m$, while under the melting point, they show increasing deviation with decreasing temperature (the solubilities are higher than predicted by the thermodynamic equation). The difference originates from the inherent nature of these substances that they form supercooled liquids and/or different crystal modifications after cooling from the melt. The heat content remains relatively high, decreasing the energy term in eq. (12).

The solubility of the two self-associating molecules, AO4 and AO5, differs considerably from the thermodynamically predicted values in both temperature ranges, as can be seen from Figure 15. At $T \ll T_m$, the solubilities are higher, and at $T > T_m$, lower than expected. In the case of these materials, two effects of opposite directions are

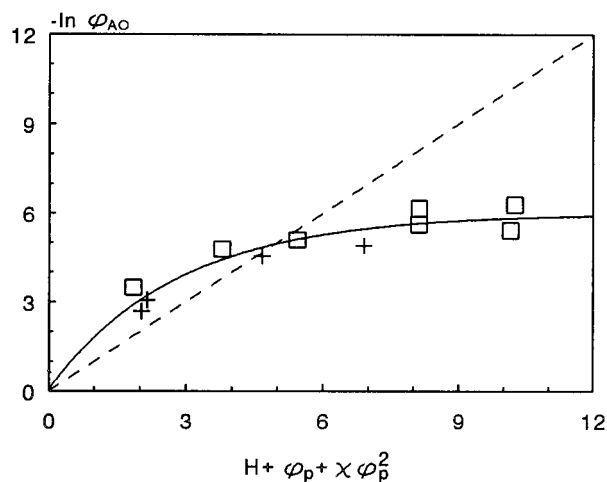


Figure 15 Thermodynamic evaluation of additive solubility in PBD: (□) AO4; (+) AO5.

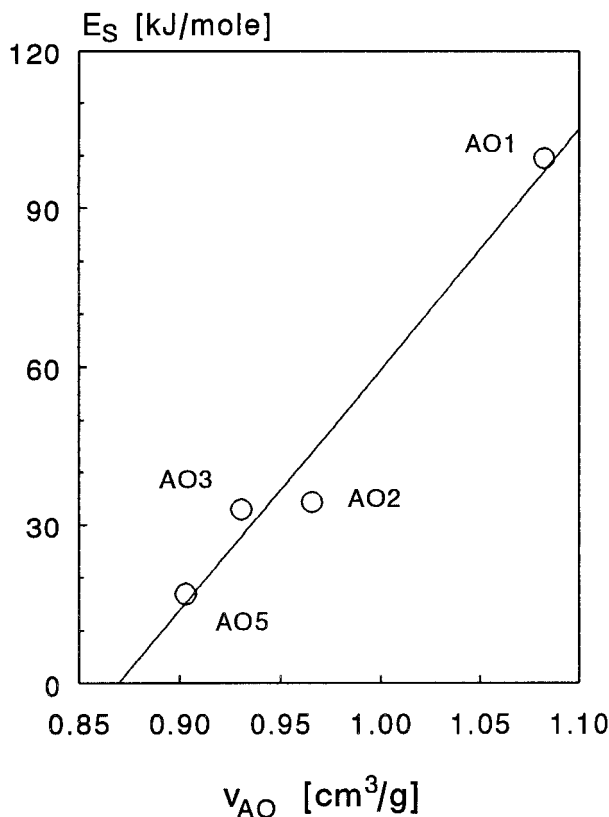


Figure 16 Effect of the specific volume of additive (measured at 25°C) on the activation energy of solubility (heat of solution).

competing. As these substances do not crystallize after melting and cooling, their heat content is higher in the additive source than in the crystalline state (resulting in increased solubility under T_m). On the other hand, these antioxidants form hydrogen bonds, which seem to be not completely dissociated even at relatively high temperatures, decreasing the solubility above T_m . The solubility parameter calculated from the molar attraction constants does not take into account the interaction forces of hydrogen bonds; therefore, the Flory-Huggins interaction parameter calculated by eq. (13) is smaller than the effective value. The sum of structural and interaction effects yields a saturation curve crossing the theoretical line in the temperature range somewhere below the melting point of the AO.

The solubility of four of the five additives investigated varies exponentially with reciprocal temperature. According to the van't Hoff relationship, the activation energy of molar solubility equals the heat absorbed on dissolution.²⁷ The influence of the effective size of additives on the heat of solution was examined by plotting E_s as a func-

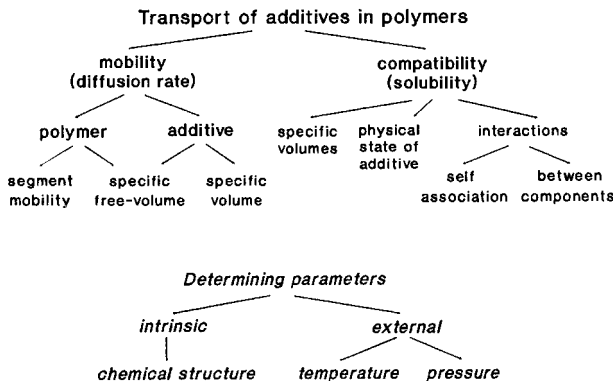


Figure 17 Parameters determining the transport of additives in polymers.

tion of specific volumes measured at 25°C in Figure 16. The increase of the activation energy with U_{AO} reveals that the specific volume of the additive strongly affects the solubility in PBD. We can conclude that the solubility of additives are influenced by the specific volume and the physical state of the additive, the interaction between components, as well as the strength of self-association of the dissolving molecules.

CONCLUSIONS

Compatibility of five primary AO with PBD was studied in a wide temperature range. The diffusion coefficient and solubility were determined by "sorption techniques." Quantitative relationships were found between the characteristics of the components and the parameters describing the transport properties. The qualitative picture drawn as a conclusion is shown in Figure 17.

1. The AO swell PBD. The free volume of the system equals the sum of the free volumes of polymer and additive. The diffusion rate is determined by the specific volume of the diffusant, the total free volume of the system, as well as the mobility of the polymer chain segments.
2. The solubility of additives in PBD depends on the specific volume, physical state, and self-association of the AO in addition to the strength of the polymer/additive interaction.
3. The solubility of AO above their melting point can be characterized by the thermodynamic parameters, in case the substance does not form hydrogen bonds. Below the melting point, the thermodynamic theory

of solution of solids can be applied only in certain cases, as most of the additives are polymorphous materials. Their physical state can depend on the surrounding medium and the thermal history of the system.

4. No surface blooming was observed in cases where sufficient additive was included to cause supersaturation. The additives remained essentially within the polymer bulk.

The authors are indebted to General Electric Plastics and to the National Scientific Research Foundation of Hungary (Grant No. OTKA T-019425) for the financial support of this work, as well as to Ciba-Geigy Ltd. for providing the additive samples. They express their thanks to Béla Turcsányi for advising and helping in the mathematical treatment of data, to Dr. Jean-Francois Guillard, as well as to Mária Sinka and Judit Szauer for their contribution in the experimental work.

APPENDIX: COMMERCIAL NAMES OF THE INVESTIGATED ADDITIVES

AO1	Irganox 1076
AO2	Irganox 259
AO3	Irganox 1010
AO4	Irganox 1098
AO5	Irganox 245

REFERENCES

1. E. Földes, *Polym. Degrad. Stab.*, **49**, 57 (1995).
2. M. Suzuki and C. A. Wilkie, *Polym. Degrad. Stab.*, **47**, 217 (1995).
3. P. G. Kelleher, D. J. Boyle, and B. D. Gesner, *J. Appl. Polym. Sci.*, **11**, 1731 (1967).
4. T. Hirahi, *Jpn. Plast.*, **Oct**, 22 (1970).
5. D. M. Kulich and M. D. Wolkowicz, ACS Advances in Chemistry Series, 222, American Chemical Society, Washington, DC, 1989, p. 329.
6. D. M. Kulich, M. D. Wolkowicz, and J. C. Wozny, *Makromol. Chem. Macromol. Symp.*, **70/71**, 407 (1993).
7. J. Crank, *The Mathematics of Diffusion*, Clarendon Press, Oxford, 1975.
8. A. R. Berens and H. B. Hopfenberg, *Polymer*, **19**, 489 (1978).
9. A. K. Doolittle, *J. Appl. Polym. Sci.*, **22**, 1471 (1951).
10. R. Chiang and P. J. Flory, *J. Am. Chem. Soc.*, **93**, 2857 (1961).
11. D. R. Paul and A. T. DiBenedetto, *J. Polym. Sci. Part C*, **10**, 17 (1965).

12. R. H. Gee and R. H. Boyd, *Polymer*, **36**, 1435 (1995).
13. G. Socrates, *Infrared Characteristic Group Frequencies*, Wiley, Chichester, 1980.
14. E. Földes and B. Turcsányi, *J. Appl. Polym. Sci.*, **46**, 507 (1992).
15. M. Dubini, O. Cicchetti, G. P. Vicario, and E. Bua, *Eur. Polym. J.*, **3**, 473 (1967).
16. R.-J. Roe, H. E. Bair, and C. Gieniewski, *J. Appl. Polym. Sci.*, **18**, 843 (1974).
17. N. C. Billingham, in *Oxidation Inhibition in Organic Materials*, Vol. 2, J. Pospíšil and P. P. Klemchuk, Eds., CRC Press, Boca Raton, FL, 1990, Chap. 6, p. 249.
18. K. Möller and T. Gevert, *J. Appl. Polym. Sci.*, **51**, 895 (1994).
19. V. Dudler and C. Muiños, ACS Advances in Chemistry Series 249, American Chemical Society, Washington, DC, 1996, p. 441.
20. S. H. Nah and A. G. Thomas, *J. Polym. Sci. Polym. Phys. Ed.*, **18**, 511 (1980).
21. M. J. R. Loadman, *Natl. Rubb. Technol.*, **16**, 69 (1985).
22. E. Földes, *Polym. Bull.*, **34**, 93 (1995).
23. M. H. Cohen and D. Turnbull, *J. Chem. Phys.*, **31**, 1164 (1959).
24. M. Hedenqvist, A. Angelstok, L. Edsberg, P. T. Larsson, and U. W. Gedde, *Polymer*, **37**, 2887 (1996).
25. J. H. Hildebrand and R. L. Scott, *The Solubility of Non Electrolytes*, 3rd ed., Reinhold, New York, 1950.
26. K. L. Hoy, *J. Paint Technol.*, **42**(541), 76 (1970).
27. E. A. Moelwyn-Hughes, *Physical Chemistry*, 2nd ed., Pergamon, Oxford, 1961.